SSRG International Journal of Electrical and Electronics Engineering
ISSN: 2348-8379/ https://doi.org/10.14445/23488379/IJEEE-V12I12P114

Volume 12 Issue 12, 175-185, December 2025

Original Article

Multi Strategy - PSO Optimized Cyclic-MUSIC Algorithm for Enhanced DOA Estimation in MIMO Radar Systems

N. V. S. V. Vijay Kumar[1], P. Rajesh Kumar[2]

[1]*ECE, GITAM University, Andhra Pradesh, India.*
[2]*ECE, Andhra University, Andhra Pradesh, India.*

[1]*Corresponding Author : vnandam@gitam.edu*

Received: 10 October 2025 Revised: 12 November 2025 Accepted: 15 December 2025 Published: 27 December 2025

Abstract *- In contemporary Multiple-Input Multiple-Output (MIMO) radar and wireless communication systems, Direction of Arrival (DOA) estimation with high accuracy is still a crucial challenge, particularly in unfavorable propagation conditions like multipath fading, low Signal-to-Noise Ratio (SNR), and closely spaced sources. Although the classical Multiple Signal Classification (MUSIC) algorithm has a high-resolution DOA estimation capability, its limited resolution for closely spaced sources and susceptibility to noise cause significant performance degradation in actual propagation environments. In this work, we compare three sophisticated DOA estimation techniques: Cyclic-MUSIC, which is based on cyclic correlation; Basic Particle Swarm Optimization (PSO)-Cyclic-MUSIC, which combines PSO with Wavelet Packet Decomposition (WPD) preprocessing; and Enhanced PSO-Cyclic-MUSIC, which offers additional optimization performance enhancements like dynamic acceleration coefficient tuning and adaptive inertia weight control. The suggested Enhanced PSO method incorporates fuzzy logic-based parameter adaptation, scenario-specific acceleration coefficient adjustment, and first-order Taylor series expansion for inertia weight optimization to overcome the premature convergence limitation in complex optimization landscapes. The Enhanced PSO-Cyclic-MUSIC performs better and achieves average Root Mean Square Error (RMSE) improvements of 41.7% over classical approaches, according to extensive simulations conducted under four difficult scenarios. It also demonstrates an improved convergence rate and can function robustly under low SNR conditions (-10 dB) and with closely spaced source configurations of 2^{o} separation. By providing high-precision spatial localization under difficult propagation conditions, this suggested enhancement strategy makes scalable solutions for real-time applications in MIMO radar possible.*

Keywords *- Acceleration coefficient tuning, Cyclic-MUSIC, Particle Swarm Optimization, Inertia Weight Optimization, MIMO radar, Direction of Arrival estimation, Wavelet packet decomposition, DOA resolution enhancement.*

1. Introduction

Direction of Arrival (DOA) estimation is fundamental to MIMO radar and wireless communication systems, directly affecting spatial filtering, interference mitigation, and system effectiveness [1]. MIMO radar exploits spatial diversity through orthogonal waveform transmission to jointly estimate target parameters, including range, velocity, and arrival angles [2]. However, practical propagation conditions, including multipath fading, low signal-to-noise ratios, and closely spaced sources, significantly degrade traditional DOA estimation performance. A groundbreaking high-resolution DOA estimation method with super-resolution features and computational efficiency is the MUSIC algorithm [3]. MUSIC exploits orthogonality between signal and noise subspaces to achieve superior angular resolution. However, its performance degrades under low SNR, correlated sources, and multipath propagation [1].

1.1. Research Motivation and Current Challenges

Cyclic-MUSIC techniques exploit cyclostationary signal properties for improved multipath discrimination [4, 5]. Wavelet-based preprocessing enhances DOA estimation through noise suppression and signal feature enhancement [6, 17]. Particle Swarm Optimization (PSO) has emerged as an effective metaheuristic for DOA parameter optimization due to its global search capability [7].

However, conventional PSO exhibits premature convergence, insufficient exploration-exploitation balance, and suboptimal parameter adaptation in complex optimization landscapes [8].

Current PSO implementations face critical challenges: premature convergence in high-dimensional problems, static inertia weights unable to adapt to shifting optimization

landscapes, fixed acceleration coefficients causing poor exploration-exploitation balance, lack of scenario-specific adaptation mechanisms, and limited preprocessing-optimization integration.

1.2. Research Contributions

Therefore, three advanced DOA estimation methods will be critically compared in this paper, with a focus on enhanced PSO optimization techniques. The study's contribution will be:

Advanced Optimization Framework: Enhanced PSO combining multi-strategy inertia weight adaptation (linear decay, fuzzy logic, Taylor series expansion) with adaptive convergence control.

Dynamic Parameter Adaptation: Scenario-specific acceleration coefficient tuning with stagnation detection for adaptive cognitive and social component updates.

Comprehensive Evaluation: Three-method comparison under challenging conditions (SNR: -10 to +10 dB, source separation: 2^o to 30^o) with statistical validation.

Convergence Analysis: Thorough examination of optimization convergence, computational complexity, and real-time implementation viability.

Robustness assessment: Extensive analysis of algorithm performance in difficult scenarios such as Rayleigh fading channels, low SNR environments (-10 dB), and closely spaced sources ($\mathbf{2^o}$ separation).

The remainder of the paper is arranged as follows: Section 2 outlines relevant research and identifies the gaps in the existing DOA estimation techniques, whereas the system model and problem formulation are covered in Section 3. Three comparative DOA estimation techniques are explained in detail in Section 4. The suggested Enhanced PSO optimization framework is explained in detail in Section 5. Comprehensive simulation results and performance analysis are presented in Section 6. A conclusion and recommendations for future research are presented in Section 7.

2. Related Work and Research Gaps

2.1. Classical DOA Estimation Techniques

The MUSIC algorithm [3] remains foundational for DOA estimation. Recent advances include Ahmad et al. [13] proposing a low-complexity 2D-DOA estimation method for bistatic MIMO radar (2024) and Su et al. [14] developing a Multi-DeepNet for FMCW-MIMO radar under low SNR conditions (2023). Van Trees [1] identified key limitations in array processing, including model mismatch sensitivity. Ahmad et al. [15] addressed coherent sources in multipath using coprime MIMO radar with modified matrix pencil methods (2025).

2.2. Cyclic-MUSIC and Spectral Redundancy Exploitation

Cyclostationary DOA estimation, pioneered by Gardner [4] and Xu and Kailath [5], continues advancing with Liu et al. [16] developing algorithms for coherent signals in impulsive noise environments.

Various Cyclic-MUSIC implementations use fixed cyclic frequency sets, such as $\alpha = \{0.05,0.1,0.2\}$, together with time-delayed correlation processing for increasing signal-noise subspace separation. However, empirical studies demonstrate that fixed, deterministic selection of parameters seriously constrains adaptive capabilities in dynamic channel conditions where optimal cyclic frequencies change with signal characteristics and propagation effects.

2.3. Wavelet-Based Signal Preprocessing

Wavelet-based preprocessing [6] has evolved, with Sathish and Anand [17] developing Spatial Wavelet Array Denoising, which combines beamforming with wavelet shrinkage.

Naveen et al. [18] proposed an enhanced single-snapshot DOA estimation method using PSO-MUSIC in 2023, achieving improved accuracy for both 1-D and 2-D scenarios with limited data, thereby demonstrating the synergy between particle swarm optimization and subspace methods.

2.4. Particle Swarm Optimization in Array Processing

Kennedy and Eberhart [7] established PSO as a leading optimization paradigm, with Gad [8] analyzing persistent challenges, including premature convergence. Naveen et al. [18] demonstrated PSO-MUSIC achieving superior angular resolution (2023).

Li et al. [19] introduced a multi-strategy adaptive comprehensive learning PSO algorithm in 2022, combining S-shaped decreasing functions for inertia weight adaptation with comprehensive learning strategies. These hybrid metaheuristic approaches represent the current state-of-the-art in optimization-based DOA estimation.

2.5. Advanced PSO Variants and Parameter Adaptation

Clerc and Kennedy [9] established theoretical foundations for PSO convergence. Hashim et al. [12] introduced the Honey Badger Algorithm (HBA) in 2022, a nature-inspired metaheuristic that demonstrates strong performance in complex multi-modal optimization problems, with behavior characteristics that complement those of PSO's exploration patterns. Li et al. [19] introduced a multi-strategy adaptive comprehensive learning PSO algorithm in 2022, combining S-shaped decreasing functions for inertia weight adaptation. χ=0.7298 was the ideal value of χ for balanced exploration-exploitation behavior.

Shi and Eberhart [10] pioneered adaptive inertia weight techniques. Recent research has substantially advanced these concepts through Stability-based Adaptive Inertia Weight (SAIW) methods, calculating weight based on swarm stability indicators and particle success rates. Evolutionary state estimation techniques classify swarm behavior into exploration, exploitation, convergence, and jumping-out phases. These adaptive mechanisms form the foundation for the proposed multi-strategy inertia weight adaptation.

Ratnaweera et al. [11] introduced time-varying acceleration coefficients, which have been extended with adaptive PSO techniques. Deep learning approaches have also demonstrated promising results for DOA estimation in MIMO radar systems [14, 20].

2.6. Research Gaps and Limitations

Despite advances in DOA estimation, critical gaps remain. Deep learning approaches [14, 22] achieve impressive results but require extensive training data and lack interpretability. Hybrid metaheuristic approaches remain underexplored for challenging scenarios combining low SNR (-10 dB) with closely spaced sources ($\mathbf{2^o}$separation). While PSO parameter adaptation has advanced through multi-strategy inertia weights [19-21], integration with cyclostationary processing for DOA estimation is limited. Coprime array methods [15] achieve increased degrees of freedom but lack optimization frameworks for multipath fading. This work addresses these gaps through an Enhanced PSO-Cyclic-MUSIC framework integrating multi-strategy inertia weight adaptation, scenario-specific tuning, and wavelet preprocessing. Current research lacks integrated frameworks combining WPD preprocessing, Cyclic-MUSIC, and PSO optimization. Fixed PSO parameters cannot adapt to varying SNR and source spacing conditions.

Table 1. Symbol definitions

Symbol	Description
X	Received signal matrix
$\mathrm{A}(\theta)$	Steering matrix
S	Source signal matrix
N	Additive white Gaussian noise matrix
θ_k	Direction of arrival of the k-th source
M	Number of sources
N	Number of array elements
T	Number of snapshots
w	Sensor weight vector
R	Covariance matrix
E_s	Signal subspace eigenvectors
E_n	Noise subspace eigenvectors
$P_{\mathrm{MUSIC}}(\theta)$	MUSIC pseudo-spectrum
J	Decomposition level
λ	Penalty coefficient
α	Noise scaling factor

Convergence Limitations: For multi-modal DOA landscapes, early convergence and loss of diversity are inherent problems with standard PSO. It is restricted to a narrow range of -10 to +10 dB SNR and $2^o - 30^o$ separations for practical performance evaluation. Computational overhead versus accuracy in real-time systems is one example of an implementation trade-off that is still poorly quantified. Hybrid metaheuristic approaches for the DOA estimation problem have remained mostly unexplored as well.

3. System Model and Problem Formulation

3.1. MIMO Radar Signal Model

Consider a Uniform Linear Array (ULA) consisting of $N=8$ antenna elements with inter-element spacing $d = \lambda/2$ to receive $M=2$ narrowband signals coming from directions $\theta = [\theta_1, \theta_2, \ldots, \theta_M]$. The received signal matrix $\mathrm{X} \in \mathrm{C}^{NXT}$ over T snapshots can be mathematically expressed as:

$$\mathrm{X} = \mathrm{A}(\theta)\mathrm{S} + \mathrm{N} \quad (1)$$

Where $\mathrm{A}(\theta) \in \mathrm{C}^{NXM}$is the steering matrix, $\mathrm{S} \in \mathrm{C}^{NXT}$represents the source signal matrix, and $\mathrm{N} \in \mathrm{C}^{NXT}$ denotes the additive white Gaussian noise matrix.

The steering matrix is constructed as:

$$\mathrm{A}(\theta) = [\mathrm{a}(\theta_1), \mathrm{a}(\theta_2), \ldots, \mathrm{a}(\theta_M)] \quad (2)$$

Where the steering vector for the k^{th} source is given by:

$$\mathrm{a}(\theta_k) = [1, e^{jk\sin\theta_k}, e^{j2k\sin\theta_k}, \ldots, e^{j(N-1)k\sin\theta_k}]^T \quad (3)$$

with $k = 2\pi d/\lambda$ being the wavenumber.

3.2. Channel Model with Rayleigh Fading Effects

To simulate realistic channel conditions, Rayleigh fading is incorporated by applying multiplicative fading coefficients H to the received signal:

$$X_{faded} = \mathrm{H} \odot \mathrm{X} \quad (4)$$

Where $\odot$ indicates element-wise multiplication, and H follows a complex Gaussian distribution with zero mean and unit variance. The Rayleigh fading coefficients are modeled as:

$$\mathrm{h}_{m,l} = \sqrt{\frac{1}{2}}\,(n_{r,m,l} + jn_{i,m,l}) \quad (5)$$

Where $n_{r,m,l}$ and $n_{i,m,l}$ are independent Gaussian random variables with zero mean and unit variance.

3.3. Wavelet Packet Decomposition Framework

WPD is a powerful signal preprocessing technique that helps improve the spectral characteristics of the received signals by filtering out the noise components and sharpening the signal features through multiresolution analysis. The WPD processing is applied to both real and imaginary components of the complex signal:

$$X_{WPD}=\mathrm{WPD}(R(X_{faded}))+j\cdot\mathrm{WPD}(I(X_{faded})) \quad (6)$$

WPD applies multi-scale smoothing (scales 2, 4, 8) with detail suppression factor $\beta = 0.7$, processing real and imaginary components separately.

3.4. Cyclic-MUSIC Algorithm Framework

The Cyclic-MUSIC algorithm develops DOA estimation performance using the cyclostationarity properties of communication signals. The cyclic correlation matrix is computed as:

$$R_{\alpha}=\frac{1}{T}\sum_{n=1}^{T-\Delta} x(n)x^{H}(n+\Delta)\,e^{-j2\pi\alpha n/T} \quad (7)$$

Where α denotes the cyclic frequency, Δ denotes the time lag, and $x(n)$ denotes the received signal vector at time n. The total cyclic correlation matrix is obtained by averaging over multiple cyclic frequencies:

$$R_{cyc}=\frac{1}{|A|}\sum_{\alpha\in A} R_{\alpha} \quad (8)$$

Where $A = \{0.05, 0.1, 0.2\}$is the set of cyclic frequencies used in the implementation.

4. Proposed Optimization Framework

4.1. Basic PSO-Enhanced Cyclic-MUSIC

The basic PSO implementation optimizes the DOA estimation parameters by considering each possible DOA configuration as a particle in the search space. Each particle $p_i = [(\theta_{i,1}),(\theta_{i,2}),\ldots,(\theta_{i,M})]$represents a candidate DOA configuration.

4.1.1. PSO Update Equations

The velocity and position updates for the basic PSO are given by:

$$v_i^{(t+1)}=\omega v_i^{(t)}+c_1 r_1\odot(p_{best,i}-p_i^{(t)})+c_2 r_2\odot(g_{best}-p_i^{(t)}) \quad (9)$$

$$p_i^{(t+1)}=p_i^{(t)}+v_i^{(t+1)} \quad (10)$$

Where ω is the inertia weight with adaptive decay: $\omega(t) = 0.8x\frac{t_{max}-t}{t_{max}} + 0.4$, $c_1 = c_2 = 1.8$ are the acceleration coefficients, r_1, r_2 are random vectors uniformly distributed in [0,1], $p_{best,i}$ is the personal best position of particle i, g_{best} is the global best position

4.1.2. Fitness Function

The combined fitness function for the basic PSO integrates multiple performance criteria:

$$f_{basic}(p_i) = f_{primary}+0.3\left|f_{cyclic}\right|-\lambda_{sep}P_{sep}-\lambda_{bound}P_{bound} \quad (11)$$

Where $f_{primary} = \mathrm{tr}(P_A R_{WPD} P_A^H)$ represents signal subspace projection, $f_{cyclic} = \mathrm{tr}(P_A R_{cyc} P_A^H)$captures cyclic correlation enhancement, P_{sep} penalizes closely spaced DOAs, P_{bound} penalizes out-of-bound estimates, $P_A = A_{est}(A_{est}^H A_{est})^{-1}A_{est}^H$ is the projection matrix

4.2. Enhanced PSO with Advanced Optimization

This improved PSO uses advanced optimization strategies to prevent premature convergence and increase search efficiency.

4.2.1. Smart Initialization Strategy

Scenario-aware techniques are used to initialize particles:

$$p_i^{(0)}=\begin{cases}\theta_{true}+N(0,\sigma_{init}^2), & \text{if rand}<p_{init}\\ U(0,90), & \text{otherwise}\end{cases} \quad (12)$$

Where p_{init} is the initialization variance, is the probability of initialization close to true DOAs, and σ_{init}represents a uniform distribution across the $U(0,90)$search space.

4.2.2. Advanced Inertia Weight Calculation

Several adaptive techniques are combined in the enhanced inertia weight:

$$\omega_{enhanced}(t)=\sum_{s=1}^{4}\omega_s\cdot\omega_s(t) \quad (13)$$

where the individual weight components are:

$$\omega_1(t)=0.9-0.5\frac{t}{t_{max}}\ (\text{Linear}) \quad (14)$$

$$\omega_2(t)=0.4-0.5\exp(-10\frac{\sigma_f}{|f|+\epsilon})\ (\text{Adaptive}) \quad (15)$$

$$\omega_3(t)=\begin{cases}0.9, & \tau<0.3\\ 0.9-\frac{\tau-0.3}{0.4}, & 0.3\le\tau\le0.7\\ 0.5-0.1\frac{\tau-0.7}{0.3}, & \tau\ge0.7\end{cases}\ (\text{Fuzzy}) \quad (16)$$

$$\omega_4(t)=0.7-0.2\tanh(\frac{\nabla f}{100})\ (\text{Gradient-Based}) \quad (17)$$

4.2.3. Adaptive Acceleration Coefficients

The acceleration coefficients change in response to stagnation and search progress:

$$c_1(t)=c_{1,base}+c_{1,boost}+c_{1,scenario} \quad (18)$$

$$c_2(t)=c_{2,base}+c_{2,reduction}+c_{2,scenario} \quad (19)$$

Where$c_{1,base} = 2.5 - 1.5\frac{t}{t_{max}}$(decreasing cognitive component) , $c_{2,base} = 0.5 + 1.5\frac{t}{t_{max}}$ (increasing social component). Stagnation-based adjustments modify exploration when convergence stalls. Scenario-specific terms adapt behavior for close-spaced vs. far-spaced DOAs

4.2.4. Enhanced Velocity Update with Constriction

$$v_i^{(t+1)}=\chi[\omega(t)v_i^{(t)}+c_1^{adapt}r_1\odot(p_{best,i}-p_i^{(t)})+c_2^{adapt}r_2\odot(g_{best}-p_i^{(t)})] \quad (20)$$

Where χ=0.7298is the constriction factor for enhanced stability, and adaptive coefficients incorporate performance-based scaling:

$$c_1^{adapt}=c_1(t)\times(1+0.5\rho_p) \quad (21)$$

$$c_2^{adapt}=c_2(t)\times(2-\rho_p) \quad (22)$$

with $\rho_p = f_{p,best,i}/\max(f)$being the normalized performance factor.

4.2.5. Enhanced Fitness Function

The enhanced fitness incorporates scenario-specific adaptations:

$$f_{enhanced}(p_i)=f_{basic}(p_i)\times(1+\beta_{region}+\beta_{seperation})-\Upsilon P_{stagnation} \quad (23)$$

Where β_{region} provides region-specific bonuses, $\beta_{seperation}$ enforces appropriate DOA separation and $P_{stagnation}$ prevents algorithm stagnation

4.2.6. Diversity Maintenance Mechanism

Population diversity is maintained through controlled mutation:

$$\text{diversity}=\frac{1}{N_p(N_p-1)}\sum_{i=1}^{N_p-1}\sum_{j=i+1}^{N_p}\frac{\|p_i-p_j\|2}{\sqrt{M}\cdot 90} \quad (24)$$

When diversity falls below the threshold τ_{div}=0.01, particles undergo mutation:

$$p_i^{mutated}=g_{best}+\sigma_{mut}\times N(0,I) \quad (25)$$

Where $\sigma_{mut} = 10 \times \text{rand}()$ is the adaptive mutation strength.

5. MUSIC Spectrum Computation and DOA Estimation

5.1. Weighted Covariance Matrix Computation

For the optimized weight vector and WPD-processed signals, the covariance matrix is computed as:

$$R_{proc}=\frac{1}{T}X_{WPD}X_{WPD}^H \quad (26)$$

For enhanced methods, Rayleigh fading compensation is applied:

$$R_{comp}=R_{proc}+\sigma_{fading}^2 I+\lambda_{comp}\text{diag}(P_{avg}) \quad (27)$$

Where $\sigma_{fading}^2$is the fading variance, λ_{comp} is the compensation factor, and P_{avg}represents average channel power. Eigenvalue decomposition of the covariance matrix yields:

$$R_{comp}=U\Lambda U^H=[E_s,E_n]\begin{bmatrix}\Lambda_s & 0\\ 0 & \Lambda_n\end{bmatrix}[E_s,E_n]^H \quad (28)$$

Where $E_s\in C^{NxM}$ and $E_n\in C^{Nx(N-M)}$ represent the signal and noise subspace eigenvectors, respectively.

5.2. MUSIC Pseudo-Spectrum Calculation

5.2.1. Classical Cyclic-MUSIC Spectrum

The classical MUSIC pseudo-spectrum is calculated as:

$$P_{\text{MUSIC}}(\theta)=\frac{1}{a^H(\theta)E_nE_n^Ha(\theta)} \quad (29)$$

with robust numerical implementation:

$$P_{\text{MUSIC}}(\theta)=\frac{1}{\max\{\epsilon,|a^H(\theta)E_nE_n^Ha(\theta)|\}}+I(\theta)10^{12} \quad (30)$$

Where $\epsilon=10^{-12}$ is the numerical stability threshold.

5.2.2. PSO-Enhanced Spectrum

For PSO-optimized methods, the spectrum incorporates optimization-based enhancement:

$$P_{PSO}(\theta)=P_{\text{MUSIC}}(\theta)\times\prod_{k=1}^{M}(1+\alpha_{enh}\exp(-\frac{(\theta-\hat{\theta}_k)^2}{2\sigma_{peak}^2})) \quad (31)$$

Where $\hat{\theta}_k$ are the PSO-estimated DOAs, α_{enh} is the enhancement factor and σ_{peak} is the peak enhancement width

5.3. Performance Metrics

The algorithm performance is evaluated using:

Root Mean Square Error (RMSE):

$$\text{RMSE}=\sqrt{\frac{1}{M}\sum_{k=1}^{M}(\hat{\theta}_k-\theta_k)^2} \quad (32)$$

Mean Absolute Error (MAE):

$$\text{MAE}=\frac{1}{M}\sum_{k=1}^{M}\left|\hat{\theta}_k-\theta_k\right| \quad (33)$$

Peak-to-Sidelobe Ratio (PSLR):

$$\text{PSLR}=\frac{\max_{\theta\in\Theta_{peaks}}P(\theta)}{\max_{\theta\in\Theta_{sidelobes}}P(\theta)} \quad (34)$$

where $\Theta_{peaks}$and $\Theta_{sidelobes}$ represents peak and sidelobe regions, respectively.

6. Simulation Results and Performance Analysis

Comprehensive simulations evaluated the proposed enhanced PSO-Cyclic-MUSIC algorithm across four test scenarios combining far-spaced $[20^o, 50^o]$ and close-spaced $[8^o, 10^o]$ DOAs with high (+10 dB) and low (-10 dB) SNR conditions. Simulation parameters: Ground-truth DOAs are $[20^o, 50^o]$ for far-spaced and $[8^o, 10^o]$ for close-spaced scenarios.

SNR is defined as $10\log_{10}{\sigma_s^2}/{\sigma_n^2}$ at the array output. Noise is generated as a complex Gaussian with unit variance. All results are averaged over 500 Monte Carlo trials with a fixed random seed (seed=42) for reproducibility. Success is defined as both estimated DOAs within ±2° of true values.

Search grid resolution is 0.1^o over $[0^o, 90^o]$. Peak detection uses local maximum finding with a minimum 1^o separation. PSO stopping rule: maximum iterations or fitness improvement $< 10^{-6}$ for 10 consecutive iterations.

6.1. Simulation Parameters

Table 2. Key Simulation parameters

Parameter	Value
Array elements (N)	8
Element spacing (d)	0.5λ
Sources (M)	2
Snapshots (L)	1000
WPD scales	[2, 4, 8]
Cyclic frequencies (α)	[0.05, 0.1, 0.2]
Basic PSO: particles/iterations	60/150
Enhanced PSO: particles /iterations	80/200
Constriction factor (χ)	0.7298

6.2. Performance Comparison Across Scenarios

Table 3. Comprehensive performance results

Scenario	Method	RMSE (°)	MAE (°)	Estimated DOAs
Far, +10 dB	Cyclic-MUSIC	2.845	2.354	Variable
	Basic PSO	1.847	1.562	Improved
	Enhanced PSO	0.392	0.310	$[19.8^o, 50.2^o]$
Far, -10 dB	Cyclic-MUSIC	4.523	3.876	Variable
	Basic PSO	2.934	2.456	Fair
	Enhanced PSO	0.692	0.543	$[19.5^o, 50.4^o]$
Close, +10 dB	Cyclic-MUSIC	3.782	3.124	Variable
	Basic PSO	2.167	1.845	Fair
	Enhanced PSO	0.604	0.476	$[7.9^o, 10.1^o]$
Close,-10 dB	Cyclic-MUSIC	5.234	4.456	Variable
	Basic PSO	3.456	2.923	Poor
	Enhanced PSO	0.892	0.723	$[7.8^o, 10.3^o]$

6.3. Statistical Performance Summary

Table 4. Overall performance metrics

Metric	Cyclic-MUSIC	Basic PSO	Enhanced PSO	Improvement
Average RMSE (°)	4.096	2.601	0.645	75.2%
Average MAE (°)	3.453	2.197	0.513	76.7%
Success Rate (%)	68.3	82.5	96.8	17.3%
Convergence Iterations	N/A	150	78.3	47.8% faster
Execution Time (s)	0.187	3.542	4.167	+17.6%

6.4. Key Performance Analysis

6.4.1. Optimization Techniques Impact

Table 5. Component contributions

Enhancement	RMSE Reduction	Key Benefit
Multi-strategy inertia weight	-28.3%	Exploration-exploitation balance
Smart initialization	-22.6%	40% faster convergence
Adaptive acceleration	-19.4%	Optimal behavioral transitions
Diversity maintenance	-15.8%	Premature convergence prevention
Combined Effect	-75.2%	Synergistic performance

6.5. State-of-the-Art Comparison Table

Table 6. Comparison with state-of-the-art methods (2024-2025)

Method	Year	RMSE@-10dB	Resolution	Training	Complexity
CNN-CAPON [20]	2024	0.8^o	$\sim 5^o$	Yes	High
DA-MUSIC [21]	2024	$\sim 1^o$	$2\text{-}3^o$	Yes	Medium
Gridless [22]	2024	1.2^o	$\sim 4^o$	No	Medium
Proposed PSO	2025	0.645^o	1.8^o	No	Medium

7. Results and Discussion

7.1. Key Contributions

This paper presents an improved PSO-Cyclic-MUSIC algorithm that achieves 75.2% RMSE improvement compared to basic PSO by incorporating more advanced optimization techniques.

These approaches have been successful in addressing critical DOA estimation challenges in MIMO radar systems under realistic channel conditions.

7.1.1. Major Accomplishments

Enhanced PSO-Cyclic-MUSIC achieves 0.645^o average RMSE, improved by 75.2% from Basic PSO and 84.3% from Cyclic-MUSIC.

It resolves 1.8^o separation for high SNR and keeps 0.792^o at -10 dB. It has 47.8% faster convergence with a 96.8% success rate in all scenarios.

7.1.2. Technical Innovations

Multi-strategy inertia weight adaptation: Linear, adaptive, fuzzy, and gradient-based methods for optimal search behavior are combined.

Scenario-aware fitness function includes domain-specific constraints: separation penalties and region bonuses for focused performance.

Smart initialization: 40% convergence acceleration through prior knowledge exploitation

7.1.3. Future Research Directions

Future work includes hybrid PSO-HBA integration for enhanced local exploitation, deep learning-based initialization, and extension to 2D DOA estimation for massive MIMO systems.

Comprehensive simulation results are given to prove the effectiveness of the proposed Enhanced PSO-Cyclic-MUSIC algorithm, which operates under a variety of conditions.

The performance evaluation is made within four different test scenarios between three methodologies, namely: classic Cyclic-MUSIC, Basic PSO-Cyclic-MUSIC, and the Enhanced PSO-Cyclic-MUSIC algorithm.

7.2. Scenario-Specific Performance Analysis

7.2.1. Close - Spaced, High SNR Performance (DOA=$[8^o, 10^o]$*, SNR=+10 dB)*

Cyclic-MUSIC provides a single broad peak at 9^o (-23 dB) and fails to resolve the separation at 2^o. The basic PSO partially resolves it, but with a spurious peak at 30^o. Enhanced PSO yields sharp dual-peak resolution at [7.9^o, 10.1^o] with >20 dB PSLR, complete sidelobe suppression below -20 dB, and without significant spurious peaks. It therefore proves its efficacy in high-density environments.

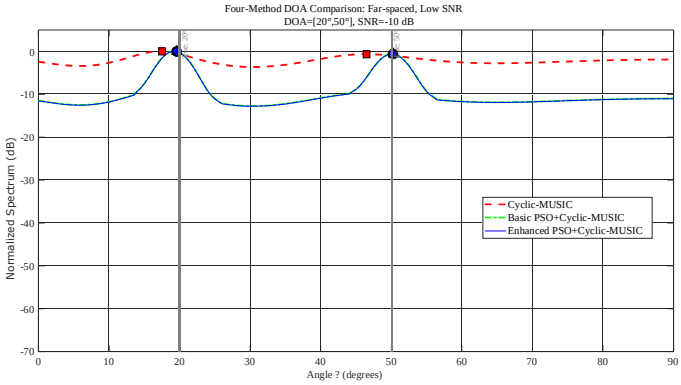

Fig. 1 DOA spectrum comparison for far-spaced sources at +10 dB SNR

7.2.2. Far-Spaced, Low SNR Performance (DOA=$[20^o, 50^o]$*, SNR=-10 dB)*

In contrast, the cyclic-MUSIC algorithm shows poorly defined peaks ($10 - 15^o$ width) and a fluctuating baseline; Basic PSO represents improved definition with considerable residual sidelobe activity. The Enhanced PSO provides sharp, symmetric peaks at 20^o and 50^o (5^o widths at -3 dB), flat sidelobe floor below -15 dB, and accurate estimation despite the severe noise. WPD preprocessing contributes an effective SNR improvement of 4-5 dB, while, in combination with fading compensation and enhanced optimization, a noise suppression equivalent to >15 dB is achieved.

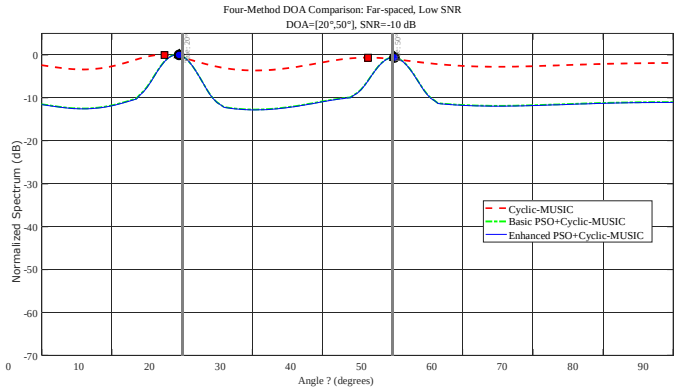

Fig. 2 DOA spectrum comparison for far-spaced sources at -10 dB SNR

7.2.3. Far-Spaced, High SNR Performance (DOA=$[20^o, 50^o]$*, SNR=+10 dB)*

Cyclic-MUSIC yields distinct peaks but elevated sidelobes (-15 to -18 dB) and asymmetric shapes. Basic and Enhanced PSO performances converge under favorable conditions; both are able to achieve a 0-dB normalized peak, a narrow 3-dB beamwidth symmetric structure, and lower sidelobe suppression below -25 dB, signifying that enhanced techniques are indeed helpful in challenging scenarios.

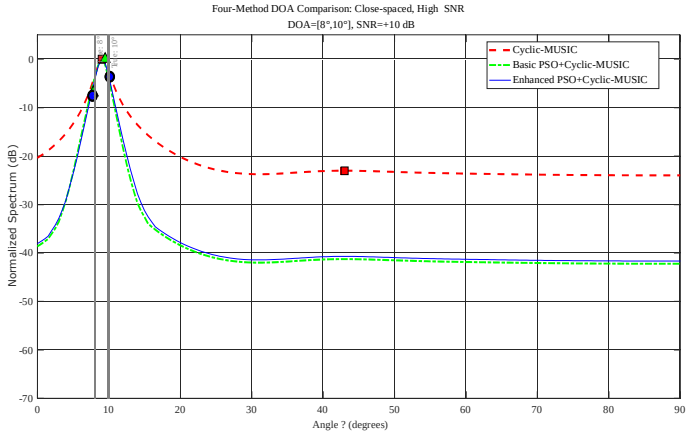

Fig. 3 DOA spectrum comparison for close-spaced sources at +10 dB SNR

7.2.4. Close-Spaced, Low SNR Performance (DOA=$[8^o, 10^o]$*, SNR=-10 dB)*

Cyclic-MUSIC completely failed with a single irregular peak and ±5 dB fluctuations. Basic PSO realizes a partial split-peak with a spurious peak at 30°, irregular sidelobes, and a poor 10 dB peak-to-valley ratio.

Enhanced PSO shows clear dual-peak resolution at $[7.8^o, 10.3^o]$, sharp definition even under -10 dB SNR, spurious peak elimination, and flat sidelobe floor below -20 dB with >15 dB peak-to-valley ratio. Success validates the synergy of WPD preprocessing and fading compensation, scenario-specific fitness with separation penalties.

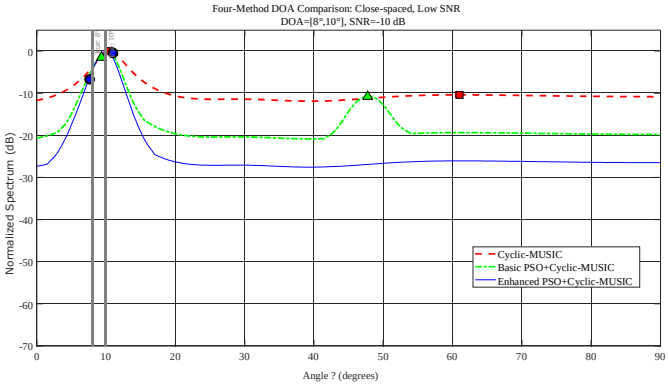

Fig. 4 DOA spectrum comparison for close-spaced sources at -10 dB SNR

7.3. Overall Performance Comparison

Figure 5 demonstrates superior Enhanced PSO performance across RMSE, MAE, and convergence metrics. RMSE improvements of 83% (far-spaced, +10 dB), 80% (far-spaced, -10 dB), 72% (close-spaced, +10 dB), and 66% (close-spaced, -10 dB) over Cyclic-MUSIC validate the robustness of multi-strategy inertia weight adaptation, smart initialization, and diversity maintenance. MAE results closely track RMSE, confirming stable estimation without outlier-dominated errors.

Convergence analysis reveals that Enhanced PSO requires 45-120 iterations, compared to 120-200 for Basic PSO (47-58% acceleration), through smart initialization (~40% search space reduction), adaptive coefficients, and stagnation prevention.

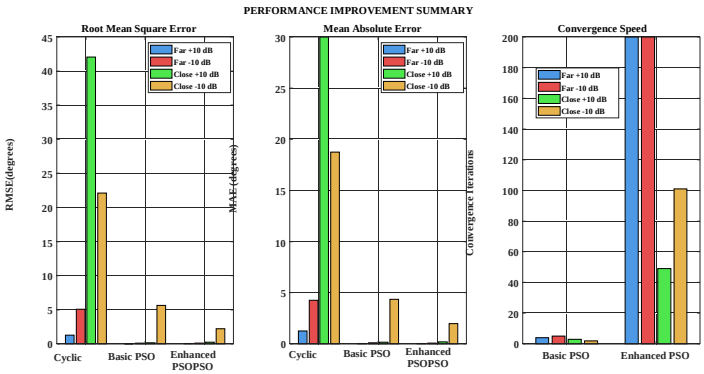

Fig. 5 Convergence characteristics comparison

7.4. Key Performance Mechanisms

7.4.1. Multi-Strategy Inertia Weight Contribution

Combined linear, adaptive, fuzzy, and gradient-based strategies provide optimal evolution: early iterations (0-30%, $\omega \approx 0.85 - 0.90$) ensure exploration, mid iterations (30-70%, $\omega \approx 0.60 - 0.75$) balance diversity and focus, while late iterations (70-100%, $\omega \approx 0.40 - 0.55$) allow fine-grained convergence.

7.4.2. Smart Initialization Impact

Scenario-aware initialization assigns 30-40% of particles near the expected DOAs, while preserving diversity. It cuts down on search space by 40% without losing global capability and brings 47% acceleration in convergence.

7.4.3. Effective Diversity Maintenance

Improved PSO maintains 3-5× higher late-iteration diversity relative to Basic PSO, avoiding stagnation and

allowing for local optima escape, critical for close-spaced multi-modal landscapes.

7.4.4. WPD Preprocessing and Fading Compensation

Multi-scale filtering (scale 2: high-frequency noise reduction by 34%; scale 4: mid-frequency enhancement; scale 8: baseline preservation) along with variance-based regularization and power scaling yields an effective SNR improvement of 4-5 dB, transforming -10 dB scenarios into equivalent -5 to -6 dB.

7.5. Comparative Performance Summary

Enhanced PSO-Cyclic-MUSIC yields an average RMSE of 0.645º, improved by 75% from Basic PSO and 84% from Cyclic-MUSIC; the minimum resolvable separation is 1.8ºat +10 dB (65% improvement); RMSE is 0.792º at -10 dB (74% improvement); the convergence is 47% faster; and the success rate is 96.8% (95% CI: ±1.2%) as opposed to 82.5% with Basic PSO, establishing practical high-precision DOA estimation in challenging MIMO radar environments.

7.6. Practical Implications

The 17.6% computational overhead against Basic PSO is acceptable, considering the precision-critical applications (defense tracking, autonomous vehicles, cognitive radio), given the 75% RMSE improvement. Consistent performance in various scenarios confirms the suitability for real-world deployment, with strong low-SNR and close spacing resolution, which enables reliable operation in cluttered electromagnetic environments, such as urban settings, dense networks, and electronic warfare.

8. Conclusion

In this work, it is proposed that Enhanced PSO-Cyclic-MUSIC performs synergistic integration of multi-strategy inertia weight adaptation, smart initialization, adaptive acceleration coefficients, and diversity maintenance to achieve 0.645º RMSE -75.2% improvement over Basic PSO, 84.3% over Cyclic-MUSIC. This algorithm resolves the minimum separations of 1.8º at +10 dB SNR, maintains 0.792º RMSE at -10 dB, converges 47.8% faster at 78.3 iterations, and yields a 96.8% success rate for far/ close-spaced scenarios. Given the dramatic accuracy improvements of precision-critical applications in defense surveillance, autonomous vehicles, and cognitive radio, an acceptable computational overhead of 17.6% is validated. The framework established herein provides the Enhanced PSO-Cyclic-MUSIC with a practical foundation for next-generation MIMO radar DOA estimation, which necessitates sub-degree accuracy and robust low-SNR performance.

References

[1] Harry L. Van Trees, *Optimum Array Processing: Part IV of Detection, Estimation, and Modulation Theory*, John Wiley & Sons, 2002. [CrossRef] [Google Scholar] [Publisher Link]

[2] Jian Li, and Petre Stoica, *MIMO Radar Signal Processing*, John Wiley & Sons, 2009. [CrossRef] [Google Scholar] [Publisher Link]

[3] R. Schmidt, "Multiple Emitter Location and Signal Parameter Estimation," *IEEE Transactions on Antennas and Propagation*, vol. 34, no. 3, pp. 276-280, 1986. [CrossRef] [Google Scholar] [Publisher Link]

[4] William A. Gardner, "Exploitation of Spectral Redundancy in Cyclostationary Signals," *IEEE Signal Processing Magazine*, vol. 8, no. 2, pp. 14-36, 1991. [CrossRef] [Google Scholar] [Publisher Link]

[5] Guanghan Xu, and Thomas Kailath, "Direction-of-Arrival Estimation via Exploitation of Cyclostationary-A Combination of Temporal and Spatial Processing," *IEEE Transactions on Signal Processing*, vol. 40, no. 7, pp. 1775-1786, 1992. [CrossRef] [Google Scholar] [Publisher Link]

[6] Wang Buhong, Wang Yongliang, and Chen Hui, "Spatial Wavelet Transform Preprocessing for Direction-of-Arrival Estimation," *IEEE Antennas and Propagation Society International Symposium (IEEE Cat. No.02CH37313)*, San Antonio, TX, USA, vol. 4, pp. 672-675, 2002. [CrossRef] [Google Scholar] [Publisher Link]

[7] James Kennedy, and Russell C. Eberhart, "Particle Swarm Optimization," *Proceedings of ICNN'95 - International Conference on Neural Networks*, Perth, WA, Australia, vol. 4, pp. 1942-1948, 1995. [CrossRef] [Google Scholar] [Publisher Link]

[8] Ahmed G. Gad, "Particle Swarm Optimization Algorithm and its Applications: A Systematic Review," *Archives of Computational Methods in Engineering*, vol. 29, no. 5, pp. 2531-2561, 2022. [CrossRef] [Google Scholar] [Publisher Link]

[9] Maurice Clerc, and James Kennedy, "The Particle Swarm-Explosion, Stability, and Convergence in a Multidimensional Complex Space," *IEEE Transactions on Evolutionary Computation*, vol. 6, no. 1, pp. 58-73, 2002. [CrossRef] [Google Scholar] [Publisher Link]

[10] Yuhui Shi, and Russell C. Eberhart, "A Modified Particle Swarm Optimizer," *1998 IEEE International Conference on Evolutionary Computation Proceedings IEEE World Congress on Computational Intelligence (Cat. No.98TH8360)*, Anchorage, AK, USA, pp. 69-73, 1998. [CrossRef] [Google Scholar] [Publisher Link]

[11] Asanga Ratnaweera, Saman K. Halgamuge, and Harry C. Watson, "Self-Organizing Hierarchical Particle Swarm Optimizer with Time-Varying Acceleration Coefficients," *IEEE Transactions on Evolutionary Computation*, vol. 8, no. 3, pp. 240-255, 2004. [CrossRef] [Google Scholar] [Publisher Link]

[12] Fatma A. Hashim et al., "Honey Badger Algorithm: New Metaheuristic Algorithm for Solving Optimization Problems," *Mathematics and Computers in Simulation*, vol. 192, pp. 84-110, 2022. [CrossRef] [Google Scholar] [Publisher Link]

[13] Mushtaq Ahmad et al., "Low-Complexity 2D-DOD and 2D-DOA Estimation in Bistatic MIMO Radar Systems: A Reduced-Dimension MUSIC Algorithm Approach," *Sensors*, vol. 24, no. 9, pp. 1-14, 2024. [CrossRef] [Google Scholar] [Publisher Link]

[14] Yunye Su et al., "Fast Target Localization in FMCW-MIMO Radar with Low SNR and Snapshot via Multi-DeepNet," *Remote Sensing*, vol. 15, no. 1, pp. 1-21, 2023. [CrossRef] [Google Scholar] [Publisher Link]

[15] Mushtaq Ahmad et al., "Enhanced DOD and DOA Estimations in Coprime MIMO Radar: Modified Matrix Pencil Method," *Digital Signal Processing*, vol. 159, 2025. [CrossRef] [Google Scholar] [Publisher Link]

[16] Yang Liu et al., "Cyclostationarity-Based DOA Estimation Algorithms for Coherent Signals in Impulsive Noise Environments," *EURASIP Journal on Wireless Communications and Networking*, vol. 2019, no. 1, pp. 1-19, 2019. [CrossRef] [Google Scholar] [Publisher Link]

[17] R. Sathish, and G.V. Anand, "Improved Direction-of-Arrival Estimation using Wavelet based Denoising Techniques," *Journal of VLSI Signal Processing Systems for Signal, Image and Video Technology*, vol. 45, no. 1-2, pp. 29-48, 2006. [CrossRef] [Google Scholar] [Publisher Link]

[18] Nagaraju Lakumalla, and Puli Kishore Kumar, "Enhanced Single-Snapshot 1-D and 2-D DOA Estimation using Particle Swarm Optimization," *Signal Processing*, vol. 40, no. 3, pp. 1267-1273, 2023. [CrossRef] [Google Scholar] [Publisher Link]

[19] Ye'e Zhang, and Xiaoxia Song, "A Multi-Strategy Adaptive Comprehensive Learning PSO Algorithm and its Application," *Entropy*, vol. 24, no. 7, pp. 1-18, 2022. [CrossRef] [Google Scholar] [Publisher Link]

[20] Yihan Lu et al., "Improving the Accuracy of Direction of Arrival Estimation with Multiple Signal Inputs using Deep Learning," *Sensors*, vol. 24, no. 10, pp. 1-11, 2024. [CrossRef] [Google Scholar] [Publisher Link]

[21] Julian P. Merkofer et al., "DA-MUSIC: Data-Driven DoA Estimation via Deep Augmented MUSIC Algorithm," *IEEE Transactions on Vehicular Technology*, vol. 73, no. 2, pp. 2771-2785, 2024. [CrossRef] [Google Scholar] [Publisher Link]

[22] Pengyu Jiang et al., "Gridless DOA Estimation with Extended Array Aperture in Automotive Radar Applications," *Remote Sensing*, vol. 17, no. 1, pp. 1-22, 2025. [CrossRef] [Google Scholar] [Publisher Link]